

P
2 mi

NG-R-31.001-46
ATS-16592

**FREE VIBRATIONS OF A PLATE
WITH VARYING NUMBER OF SUPPORTS**

by

J. Drake, C.-K. Kang, and
E. H. Dowell

Reproduced by
**NATIONAL TECHNICAL
INFORMATION SERVICE**
US Department of Commerce
Springfield, VA. 22151

November 1973

PRINCETON UNIVERSITY
Department of Aerospace and Mechanical Sciences
The Aeroelasticity and Magnetoelasticity Laboratory



AMS Report No. 1133

PRICES SUBJECT TO CHANGE

(NASA-CR-138681) FREE VIBRATIONS OF A
PLATE WITH VARYING NUMBER OF SUPPORTS
(Princeton Univ.)

N74-28362

CSSL 20K

G3/32

Unclas
16592

47P

I

FREE VIBRATIONS OF A PLATE
WITH VARYING NUMBER OF SUPPORTS

by

J. Drake, C.-K. Kang, and
E. H. Dowell

November 1973

The Aeroelasticity and Magnetoelasticity Laboratory

AMS Report No. 1133

ACKNOWLEDGEMENTS

The authors would like to thank T. R. Leuner and Professor R. Mark for useful discussions concerning this work. The research was supported by NASA Grant NGR 31-001-146.

TABLE OF CONTENTS

	<u>Page</u>
Acknowledgements	i
Table of Contents	ii
I. Introduction	1
II. Experiment	2
II.1 Method	2
II.1.1 Apparatus	2
II.1.2 Holographic Technique	2
II.2 Results	6
III. Correlation of Theory and Experiment	9
IV. Conclusions	11
References	12
List of Tables and Figures	13

I. INTRODUCTION

The purpose of this experimental investigation was to test the accuracy of an analysis which predicts the natural frequencies of vibration of a plate constrained by an arbitrary number of point supports along the edges, and to determine the number of such supports which approximates an infinite number.

II. EXPERIMENT

II.1 Method

II.1.1 Apparatus

The test specimen was a rectangular aluminum plate (8" x 8" x 1/8") which was driven by an electromagnetic oscillator and suspended by a system which approximated rigid point supports. The experimental apparatus was much the same as that employed by Leuner,¹ with modifications for point supports along the edges, (see Figs. 1, 2, 3). The corner supports are identical to those in Leuner¹. The edge supports consist of 1/4" x 1/4" x 7" beams "vee-grooved" at one end to a point and recessed to ninety degrees. These beams receive the plate edge which is bevelled to a seventy degree angle, (see Fig. 3).

The principal means of natural mode identification was by means of holography as described below.

II.1.2 Holographic Technique

For a theoretical discussion of holographic interferometry and a discussion of holographic technique see Leuner.¹ What follows is meant as a supplement to that discussion, to which one correction is offered.

From Leuner¹ page 22

The reference beam from the eight milliwatt laser was adjusted to be approximately 30% more intense than the reflected object beam (readings of 12 and 9 respectively on a Goffen Luna Pro light meter).

Readings of 12 and 9 on a Goffen Luna Pro light meter correspond approximately to 32 and 4 foot candles respectively, so that the reference beam was in fact 700% more intense than the reflected object beam. In an earlier report it

was stated that clear and bright holograms were obtained consistently when the reference and object beam intensities were approximately equal (readings of 10.7 and 9.7 respectively on a Goffen Luna Pro light meter). These readings correspond to 14 and 7 foot candles respectively so that the reference beam was in fact 100% more intense than the reflected object beam. These corrections arise from the faulty assumption that the units on the Goffen Luna Pro light meter are linear.

Approximately one hundred and forty time average holograms and 10 real time holograms have been made yet, in spite of this experience, there lingers considerable uncertainty as to the optimum holographic technique. Some optical arrangements worked well and others did not. What follows are a few hints to someone who might work with a similar apparatus for similar purposes, preceded by a discussion of the optical arrangement which worked the best.

A trend which emerged was that clear and bright holograms appeared consistently when there was an even distribution of light over the surface of the photographic plate and when the object beam was half the reference beam intensity and of sufficient intensity to give a bright image; however there were a number of exceptions to this trend. The optical arrangement that worked best is diagrammed in Fig. 4. The photographic plate is 14 1/2" from the object. For most holograms the object beam intensity was approximately 7 foot candles, the reference beam intensity was approximately 14 foot candles, and the exposure time was about 45 seconds. A difference of one or two foot candles in intensity of the beams or of 5 seconds in the exposure time made no noticeable difference.

The reference and object beam intensities used were a bit arbitrary. For this arrangement 7 foot candles was as bright as the reflected object beam would get and for the reference beam, 14 foot candles was in the region of intensity that was giving the best results and was arrived at with the light filters that were available. Other combinations of intensities and corresponding exposure times did not work as well for unknown reasons. When the photographic plate holder was moved back further from the object, which reduced the object beam intensity and changed the angle between the object and reference beams, the quality of the holograms deteriorated.

The following are hints to someone using a similar apparatus for similar purposes.

Path Length - It is recommended that the path lengths of the object and reference beams be within a centimeter; however good holograms were made with a path difference of as much as an inch.

Illumination - Getting an even distribution of light over the object is important because only parts of the object that are illuminated well are visible upon reconstruction; however producing an even distribution of light over the photographic plate with the reference beam is more critical. If the reference beam varies substantially in intensity over the surface of the photographic plate, then certain areas are going to be either over or under exposed, and the plate will contain "dark spots" through which the reconstructed image is not visible. This results in a poor polaroid photograph.

Spatial Filter - The easiest method to obtain an even distribution of light intensity over the photographic plate of object is as follows.

Remove the oval piece containing the pinhole from the spatial filter and, using only the microscope lens, adjust the position of the spatial filter until the photographic plate or the object is evenly illuminated. Then replace the piece containing the pinhole and focus the beam on the pinhole.

Beam Splitter - Presumably because the rays from the front and back surfaces of the beam splitter interfere, an interference fringe divides the reflected beam at certain reflection angles and at a given angle there is a local maximum intensity. In producing maximum intensity for the reference beam it is necessary to avoid the interference fringes and to find the local maximum for a particular angle.

Dark Room - Washing the plates in hypo clearing agent and/or photoflow solution has no effect on the reconstructed image. The following steps are sufficient for processing the photographic plates; five minutes D-19 developer, rinse in water 30 seconds, five minutes in fixer, rinse in water 30 seconds, a few minutes in methanol/water solution, a few minutes in flowing water bath.

Real Time Holography - In this investigation Real Time holograms were made using the Gaertner Real-Time Holography Plateholder model R274, which develops the holograms in situ. This plate holder was placed so that the photographic plate was in the same position horizontally as in the Time Average case. The same light intensities and exposure times were used as in the Time Average case and the directions in the Gaertner manual were followed exactly. The real time hologram will withstand slight disturbances to the holographic bench (i.e. accidental jarring) without introducing

any fringe orders into the image; however any movement of, or adjustment to the object or the plate holder will introduce an unworkable number of fringe orders to the image. Because of these characteristics and because the fringe orders of a Real Time hologram are dim and "flicker", Real Time holography does not lend itself easily to recording data photographically. For any kind of quantitative or detailed picture of the mode shape a Time Average hologram is necessary. Real Time holography is meant for identifying mode shapes and studying them qualitatively. When investigating a large number of modes for one support configuration Real Time holography is really quite convenient and avoids the hit and miss tactics of Time Average methods. The best method would be to use Real Time and Time Average holography in combination, identifying the mode and adjusting to the desired amplitude of vibration with a Real Time hologram, and then recording the mode shape with a Time Average hologram.

II.2 Results

Using Real Time as well as Time Average holographic interferometry the following plate modes were identified; the first and second doubly symmetric plate modes, the first and second symmetric-antisymmetric plate modes and the first doubly antisymmetric plate mode. The frequencies of these modes were recorded for three support configurations, all with one support at each corner and the other supports evenly distributed. These configurations were of eight, sixteen, and thirty-two supports.

Examination of the graphs of Frequency versus Support Number, (Figs. 5 through 9) leads to the conclusion that the number of point supports, evenly distributed with one at each corner, which approximates an infinite number is greater than eight and less than or equal to sixteen, at least for the lower plate modes. Also, this number of supports does not appear to be

a sensitive function of the plate mode, at least for the lower plate modes.

In Figs. 10-12 sketches of mode shapes obtained from Real Time holography are drawn. In Figs. 13-15 corresponding photographs from Time Average holography are shown.

The mode identified and depicted as the first symmetric-antisymmetric plate mode actually has a number of interference fringes crossing at points where the mode line is drawn, (see 16 and 32 support config. #2) which is an inherent contradiction. However the mode coupled easily and this discrepancy is attributed to coupling effects. (Of course this may be untrue and the mode may not be the first symmetric-antisymmetric mode at all.)

The behavior of the first doubly antisymmetric mode as a function of support number (see Fig. 7) which departs from the general pattern at the eight support configuration is actually consistent with physical requirements. Since the mode shape for the first doubly antisymmetric mode is identical in the four and eight configuration, (see Leuner¹ and 8 support config. #3) and since the four supports added in the eight support configuration lie along the mode's node lines, one would not expect any change in the frequency of the mode.

The second doubly antisymmetric mode shape in the eight support configuration looks very much as though it might be a coupled version of the missing second symmetric-antisymmetric mode in the eight support configuration. However the mode was never uncoupled, and was not plotted. This explains the reason for the gap in the graph of Frequency versus Support Number for the second symmetric-antisymmetric mode, (see Fig. 9).

The frequencies of the natural modes for the four support case were identified by their sound emission and correlation with Leuner's¹ results. They were not studied holographically.

III. CORRELATION OF THEORY AND EXPERIMENT

The theoretically computed frequencies for different numbers of supported points of a square plate are given in Tables 1 through 3. As shown, the agreement with the experimental results is satisfactory. Basically, the present computer program employed the bi-section method (which is supplemented by a two-point iteration scheme) to find the eigenvalues ω^2 of the equation^{2,3}

$$|C_{ij}| \equiv \left| \sum_k \frac{\beta_{ik} \beta_{jk}}{(\omega_k^2 - \omega^2) m_k} \right| = 0$$

ω_k , m_k are the natural frequencies and generalized masses of the plate with no supports (unconstrained).

We make the following observations regarding the computations:

- a) The number of unconstrained natural modes employed should be at least equal to twice that of supported points, otherwise, the determinant $|C_{ij}|$ will be numerically very small, which renders the determination of the roots ω^2 difficult. Therefore, the number of supports allowable in the present program is limited by the capacity and accuracy of the eigenvalue program employed in generating the unconstrained natural mode shapes and frequencies.
- b) It is possible that the root-finding method will fail to locate a root of ω^2 , especially when an unconstrained (no supports) natural frequency is also a solution for the constrained (supported) case. Care must be taken in identifying the roots

found by the present program, particularly the natural frequencies. A handy check is to run each case twice, each time employing a different number of unconstrained natural modes.

IV. CONCLUSIONS

An experimental investigation has systematically studied the effect of the number of edge point supports on the natural modes of a square plate. Satisfactory correlation with theory has been shown.

REFERENCES

1. Leuner, T. R., "An Experimental-Theoretical Study of Free Vibrations of Plates on Elastic Point Supports," AMS Report No. 1052, August 1972.
2. Dowell, E. H., "Free Vibrations of a Linear Structure with Arbitrary Support Conditions," Journal of Applied Mechanics, Vol. 38, No. 3, September 1971, pp. 595-600.
3. Dowell, E. H., "Free Vibrations of an Arbitrary Structure in Terms of Component Modes," Journal of Applied Mechanics, Vol. 39, No. 3, September 1972, pp. 727-732.

LIST OF TABLES AND FIGURES

Table 1	Four Point Supports
Table 2	Eight Point Supports
Table 3	Sixteen Point Supports
Figure 1	Holographic Bench
Figure 2	Plate Support System
Figure 3	Pylon and Beam Detail
Figure 4	Optical Arrangement of Holographic Bench
Figure 5	Frequency Vs. Support Number - First Doubly Symmetric Mode
Figure 6	Frequency Vs. Support Number - First Symmetric Antisymmetric Mode
Figure 7	Frequency Vs. Support Number - First Doubly Antisymmetric Mode
Figure 8	Frequency Vs. Support Number - Second Doubly Symmetric Mode
Figure 9	Frequency Vs. Support Number - Second Symmetric-Antisymmetric Mode
Figure 10	Plate Modes - 8 Support Configuration
Figure 11	Plate Modes - 16 Support Configuration
Figure 12	Plate Modes - 32 Support Configuration
Figure 13a	Plate Modes - 8 Support Configuration
Figure 13b	Plate Modes - 8 Support Configuration
Figure 13c	Plate Modes - 8 Support Configuration
Figure 13d	Plate Modes - 8 Support Configuration
Figure 13e	Plate Modes - 8 Support Configuration
Figure 14a	Plate Modes - 16 Support Configuration
Figure 14b	Plate Modes - 16 Support Configuration

LIST OF TABLES AND FIGURES (continued)

Figure 14c	Plate Modes - 16 Support Configuration
Figure 15a	Plate Modes - 32 Support Configuration
Figure 15b	Plate Modes - 32 Support Configuration
Figure 15c	Plate Modes - 32 Support Configuration
Figure 15d	Plate Modes - 32 Support Configuration

TABLE 1
FOUR POINT SUPPORTS

<u>Experimental Data</u>		<u>Theoretical Data</u>		$\nu = .3, a/b = 1.$	
K_E	Type	Unconstrained Natural		K_T	Type
		K_T	Type		
8.65	SS	7.15	SS	7.1	SS
16.88	AS	15.9	AS	15.6	AS
		16.0			
21.1	SS	(19.4)	SS	19.4	SS
40.5	AA	39.9	AA	38.4	AA
45.48	SS	43.5	SS	44.2	SS
		48.8	AS	48.4	AS
		53.6	AS	52.3	AS
55.6	AS	67.6	AA	67.5	AA
		83.0	AS		
		85.0	AS		
		96.8	SS	94.8	SS
				106.0	AS
		111.5	AS	111.3	AS
		121.0	(SS)	121.5	(AS)
		124.0	(AS)	124.1	(AA)
		131.0	AA	127.5	AA
				138.5	AA

difficult to judge, ()

m - mass/area
D - plate stiffness
a - plate length

$$K = \left(\frac{m\omega^2 a^4}{D} \right)^{1/2}$$

A - Anti-symmetric
S - Symmetric
E - Experimental
T - Theoretical

TABLE 2
EIGHT POINT SUPPORTS

$\nu = .3, a/b = 1.$

<u>Experimental Data</u>		<u>Theoretical Data</u>			
		Unconstrained Natural Modes = 27		Modes = 36	
K_E	Type	K_T	Type	K_T	Type
19.6	SS	18.3	SS	18.15	SS
36.4	AS	34.4	AS	(34.4)	AS
39.9	AA	42.6	AA	39.8	AA
58.0	SS	64.4	SS	62.6	SS
69.1	AA	66.3	AA	63.1	
		66.5	SS	65.5	AA
		85.0	SS	69.4	
		91.5	AS	84.6	SS
		99.5	AS	90.1	AS
				92.8	
				118.0	SS
				124.1	AA
131.9	AA			127.5	AS
				132.5	SS
				137.5	AS

TABLE 3
SIXTEEN POINT SUPPORTS

$\nu = .3, a/b = 1.$

<u>Experimental Data</u>		<u>Theoretical Data</u>			
K_E	Type	Unconstrained Natural Modes = 27		Modes = 36	
		K_T	Type	K_T	Type
21.3	SS	19.9	SS	19.65	SS
49.0	AS	49.6	AS	48.4	AS
		52.2	AS	50.4	AS
72.8	AA	83.6	AA	79.0	AA
90.7	SS	100.5	(SS)	100.6	(AA)
		104.5	AA		
106.8	AS			(105.8)	AS
				127.5	AS
				128.5	
		133.2	AS	132.5	AS
		147.4	AA		

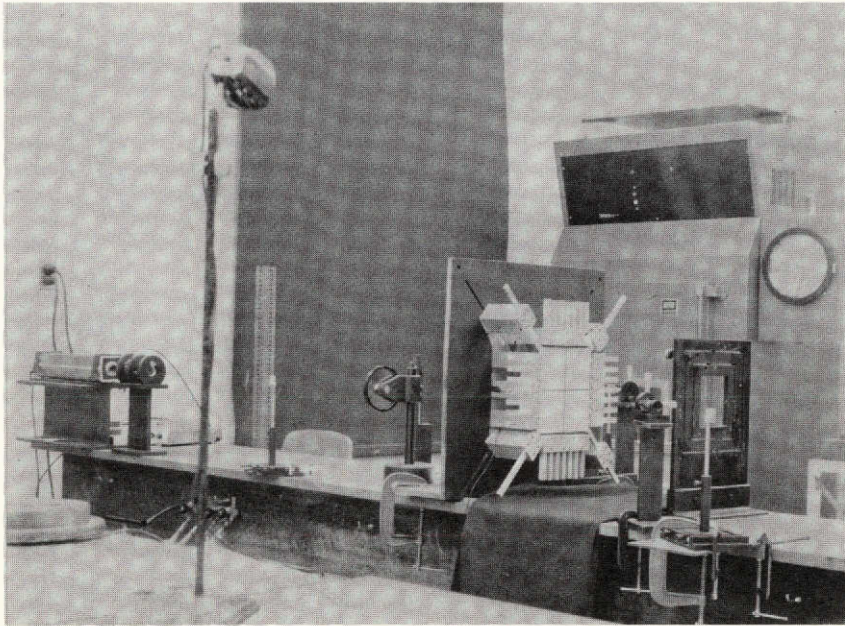


FIGURE 1. HOLOGRAPHIC BENCH

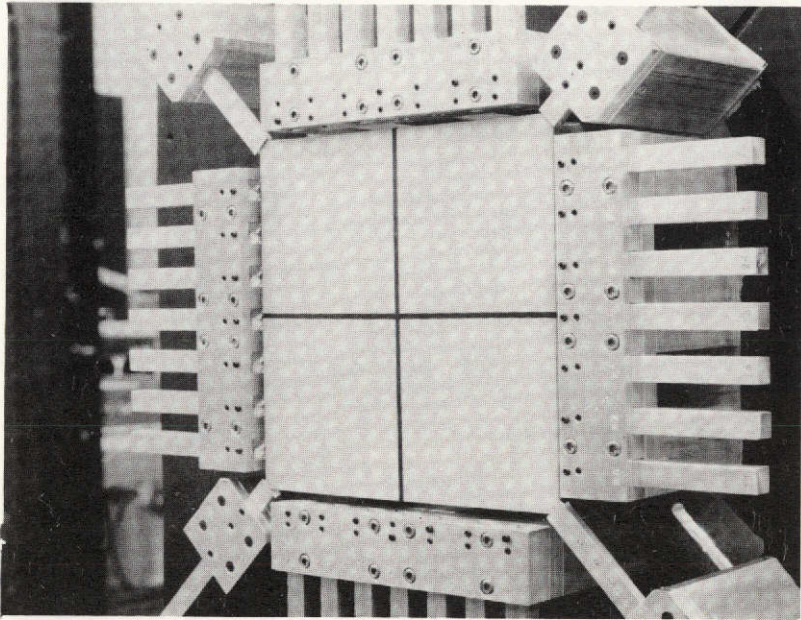


FIGURE 2. PLATE SUPPORT SYSTEM

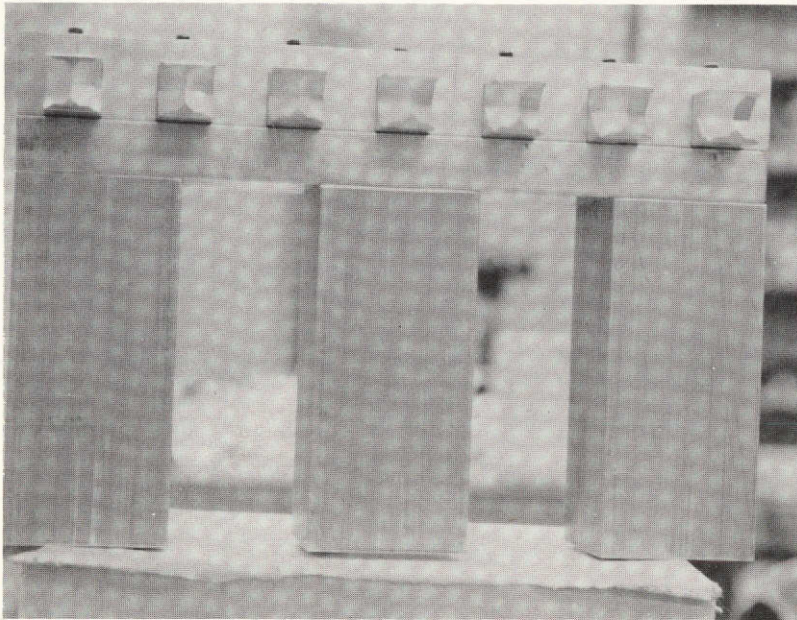


FIGURE 3. PYLON AND BEAM DETAIL

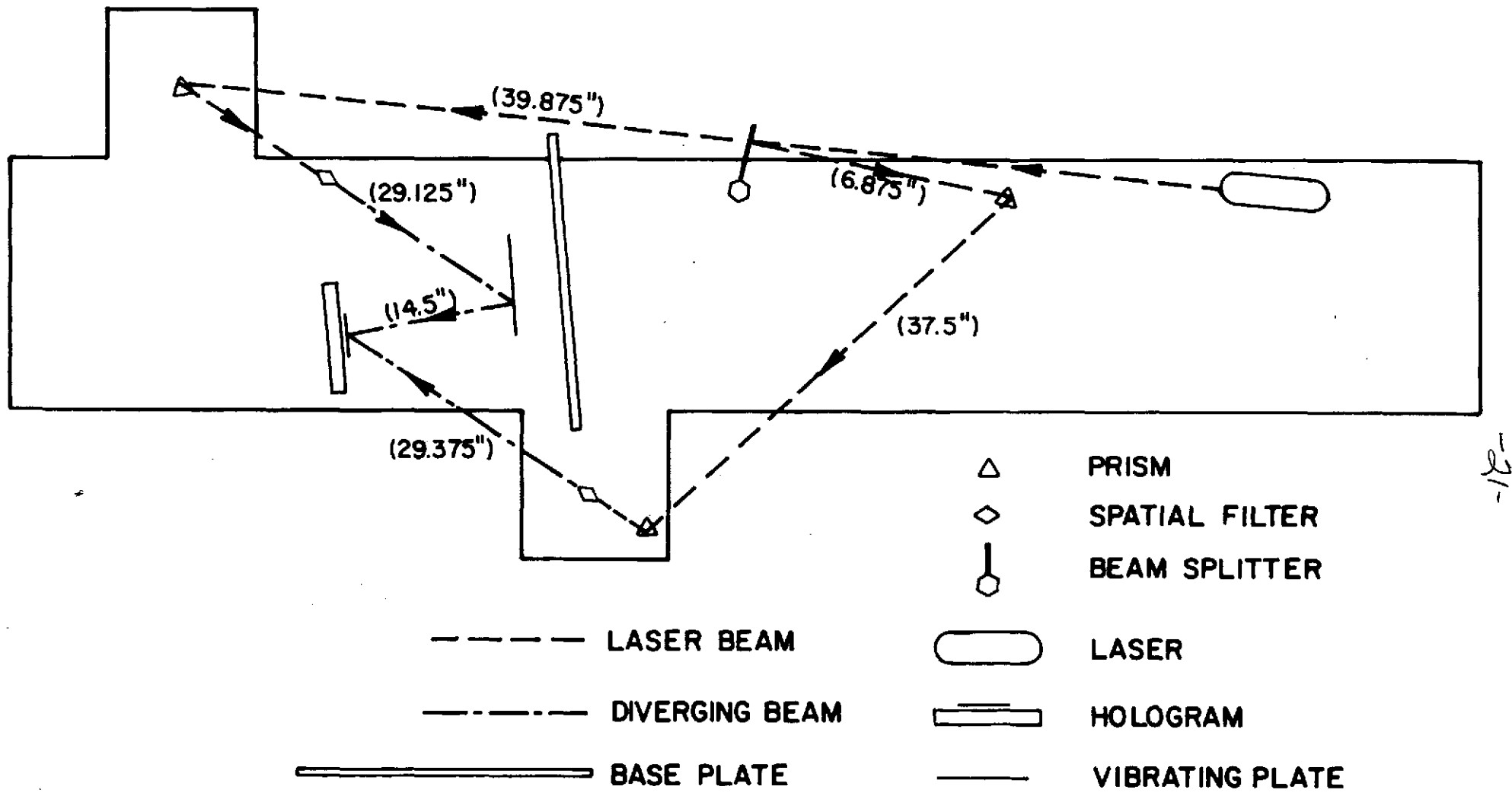


FIGURE 4. OPTICAL ARRANGEMENT OF HOLOGRAPHIC BENCH

26

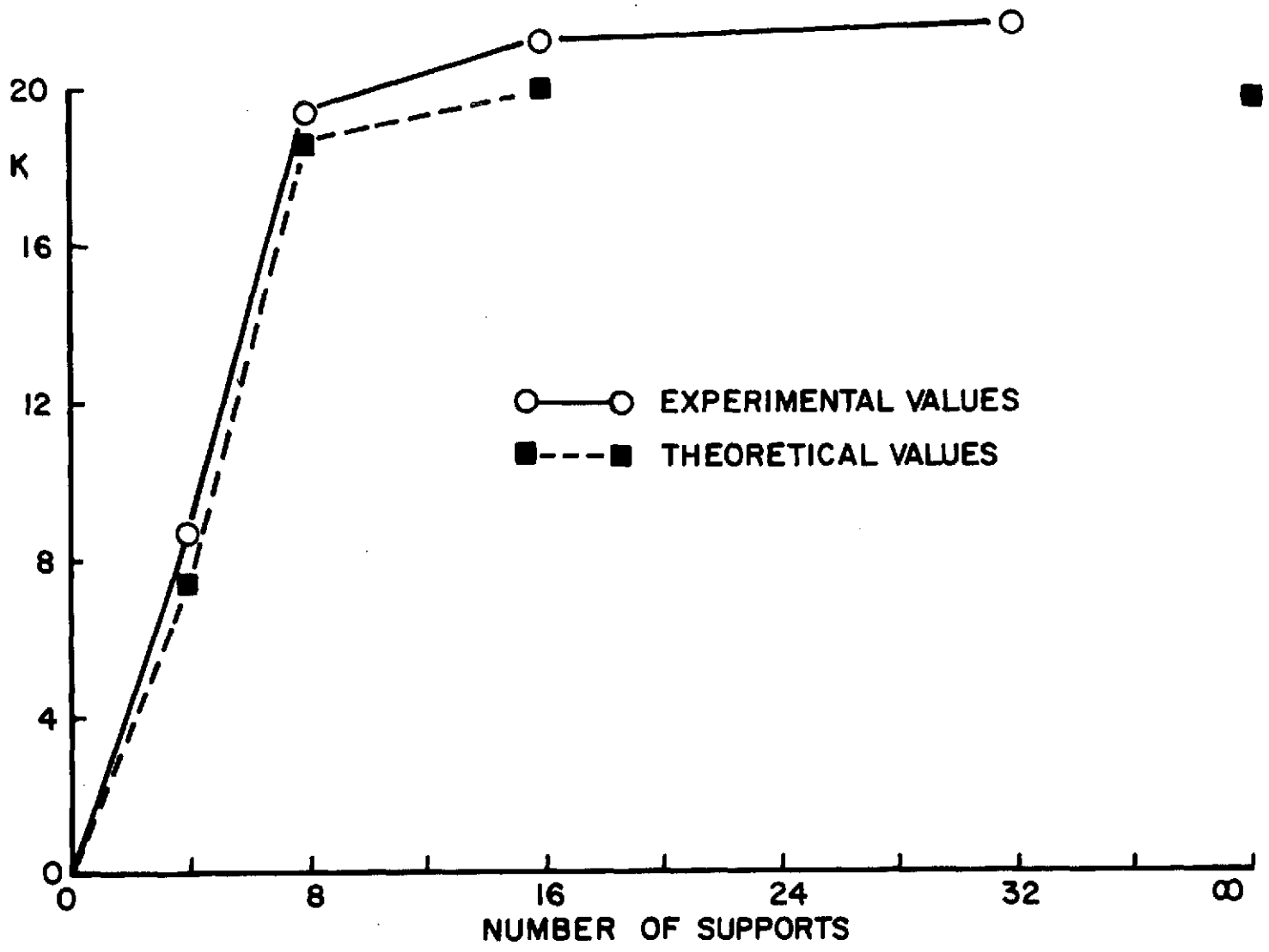


FIGURE 5. FREQUENCY VS. SUPPORT NUMBER — FIRST DOUBLY SYMMETRIC MODE

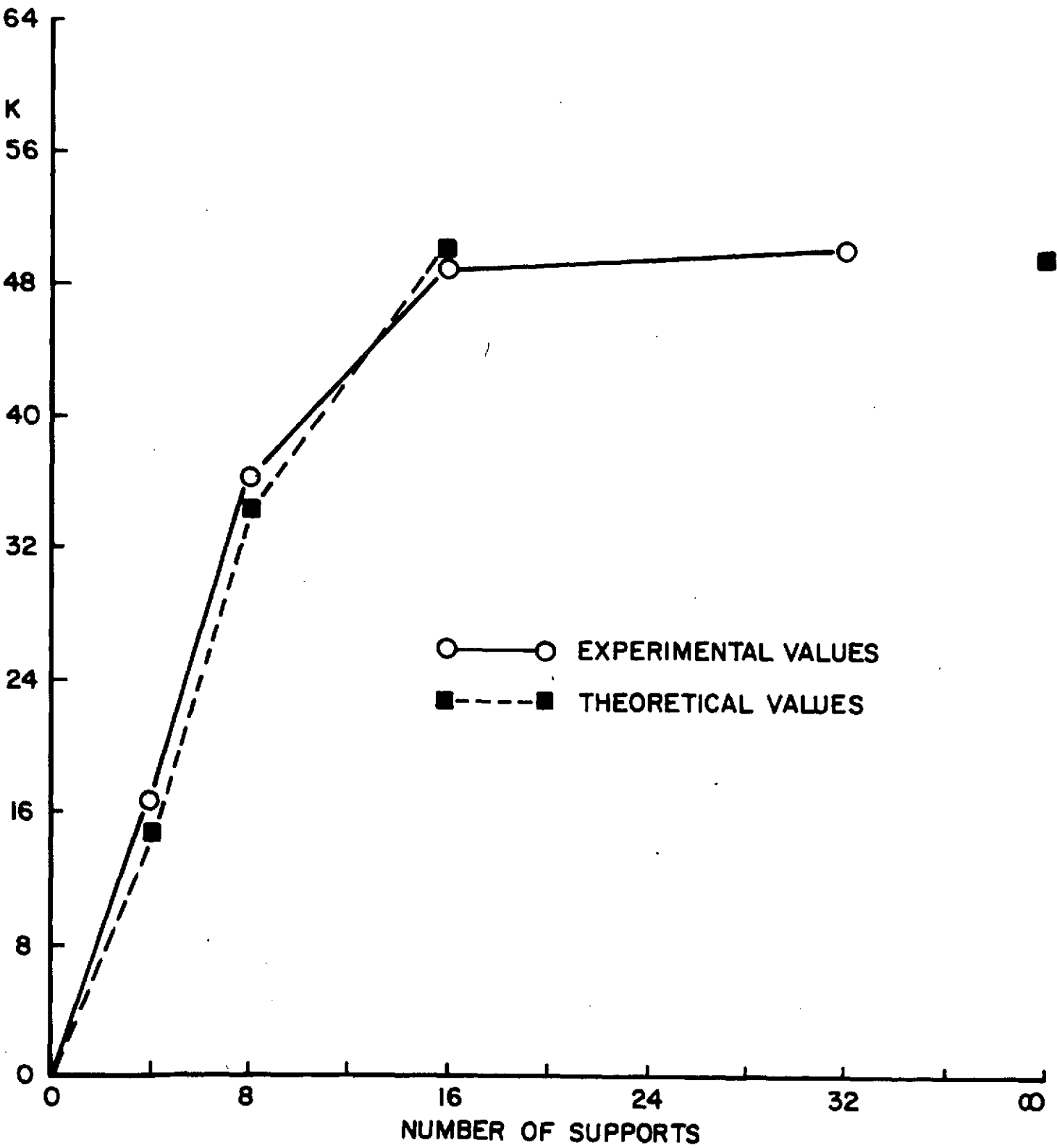


FIGURE 6. FREQUENCY VS. SUPPORT NUMBER—FIRST SYMMETRIC-ANTISYMMETRIC MODE

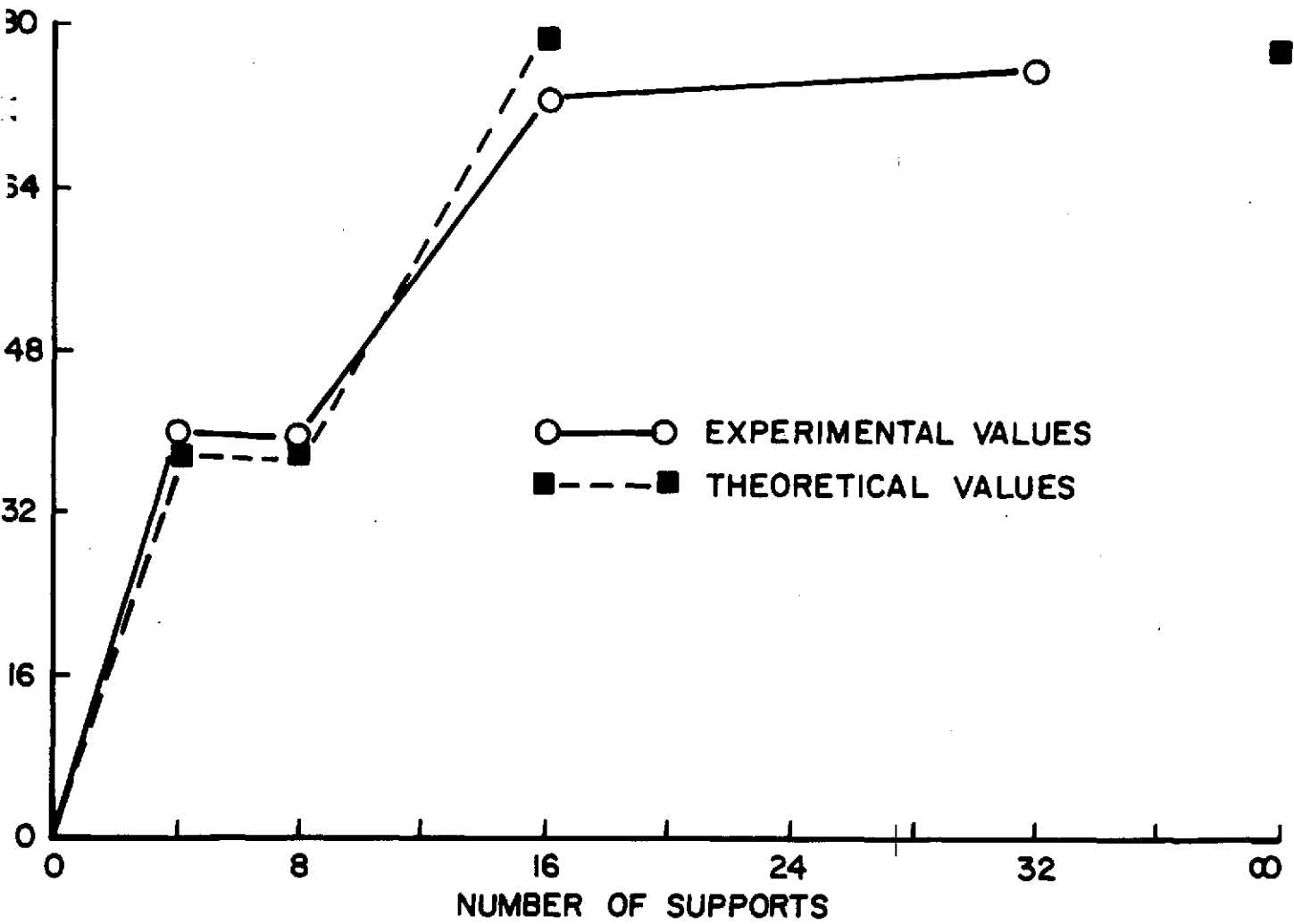


FIGURE 7. FREQUENCY VS. SUPPORT NUMBER — FIRST DOUBLY ANTISYMMETRIC MODE

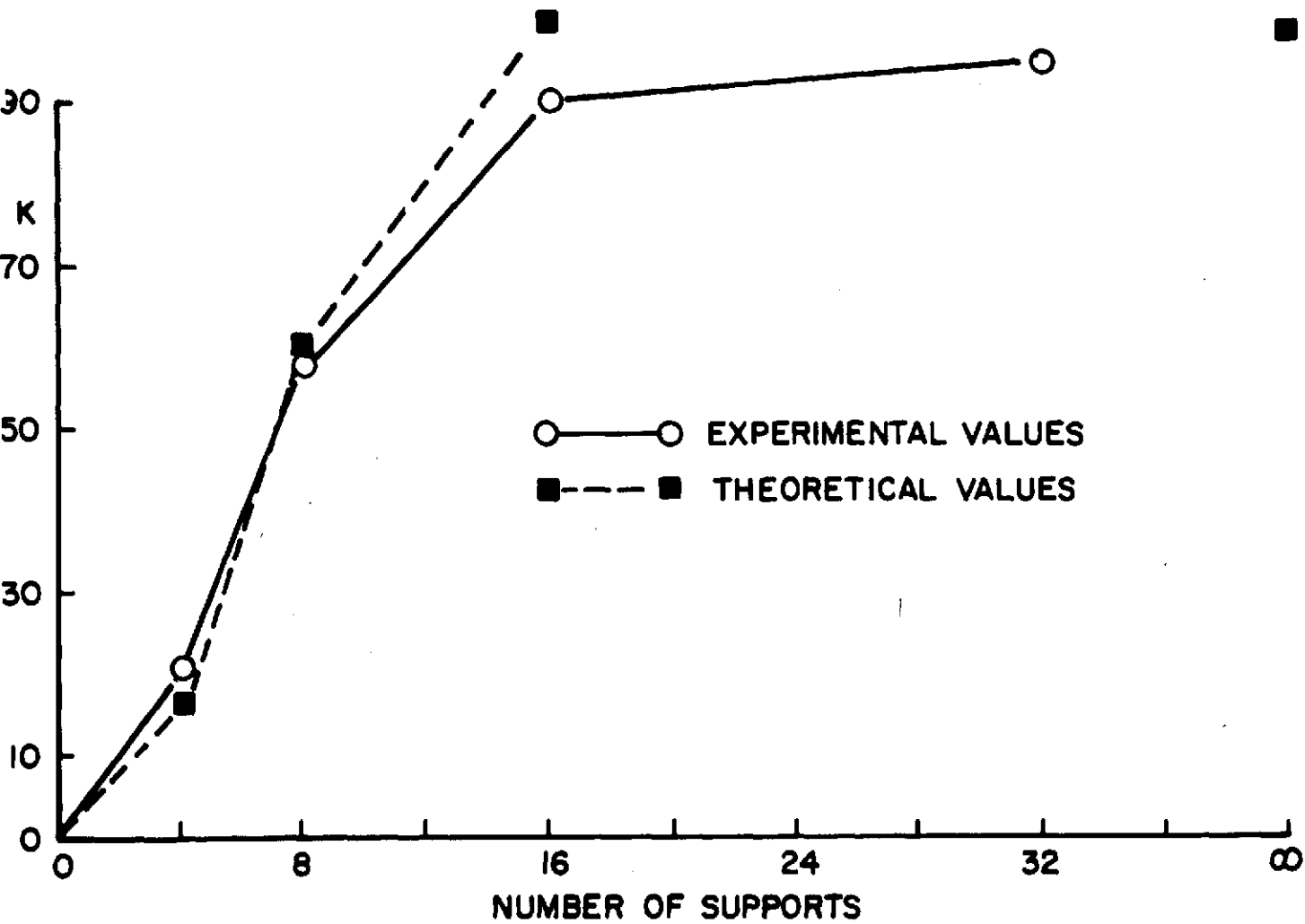


FIGURE 8. FREQUENCY VS. SUPPORT NUMBER - SECOND DOUBLY SYMMETRIC MODE

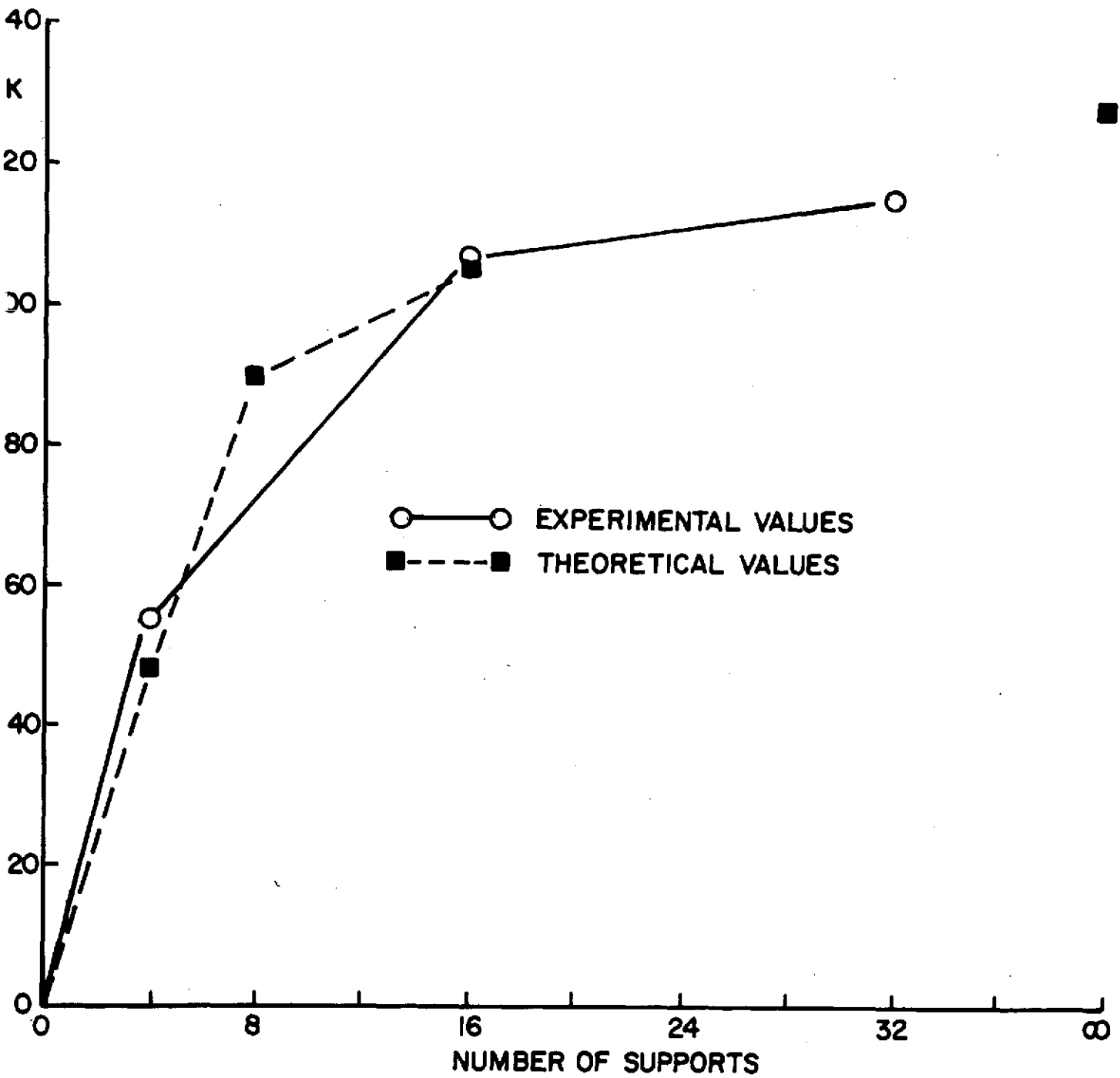
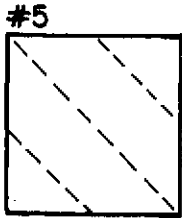
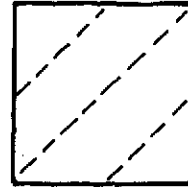


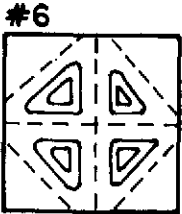
FIGURE 9. FREQUENCY VS. SUPPORT NUMBER—SECOND SYMMETRIC-ANTISYMMETRIC MODE



#5
K=69.1
DOUBLY ANTISYMMETRIC

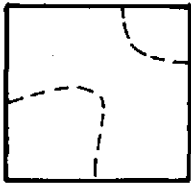


K=67.8



#6
K=131.9
DOUBLY ANTISYMMETRIC

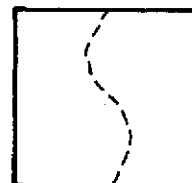
The first symmetric-antisymmetric and antisymmetric-modes couple very easily and are rarely seen uncoupled in Time Average holograms. Real Time holography enabled the change from one mode to the other to be visualized and this process is depicted below.



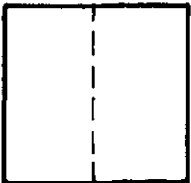
K=38.77



K=37.57



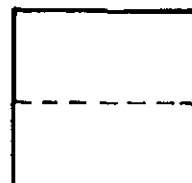
K=37.51



K=36.4



K=35.98

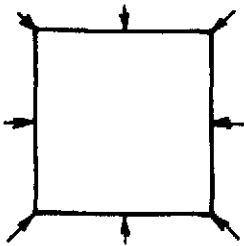


K=35.72

* It is quite possible that this mode is coupled and is really symmetric-antisymmetric, however it was never seen uncoupled.

FIGURE 10. PLATE MODES - 8 SUPPORT CONFIGURATION

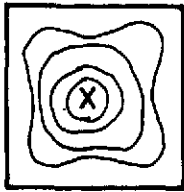
SUPPORT CONFIG.



----- NODE LINE
———— INTERFERENCE FRINGE
X ELECTROMAGNETIC EXCITER

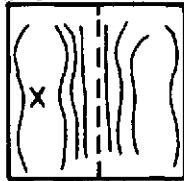
The following mode shapes were viewed during Real Time holography and recorded by sketching.

#1

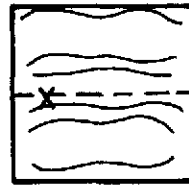


K=19.6
DOUBLY SYMMETRIC

#2

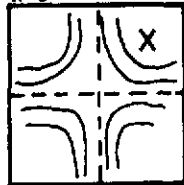


K=36.4
SYMMETRIC-ANTISYMMETRIC



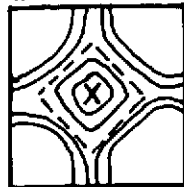
K=35.8

#3



K=39.9
DOUBLY ANTISYMMETRIC

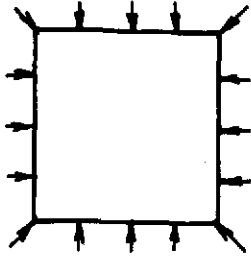
#4



K=58.
DOUBLY SYMMETRIC

FIGURE 10. PLATE MODES-8 SUPPORT CONFIGURATION (CONTINUED)

SUPPORT CONFIG.



Sketches of Real Time Observations

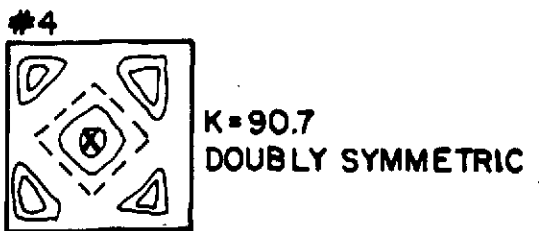
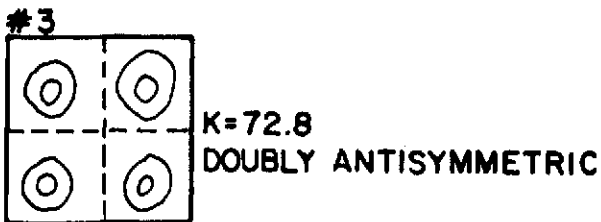
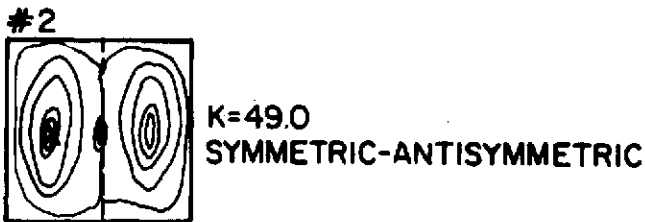
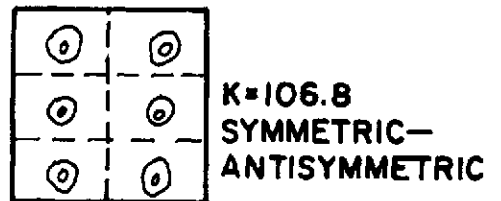
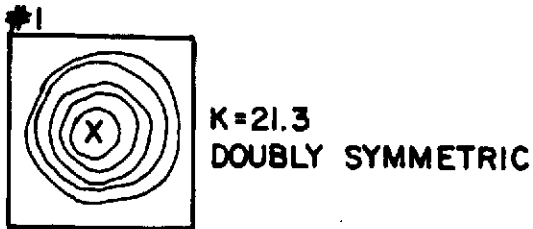
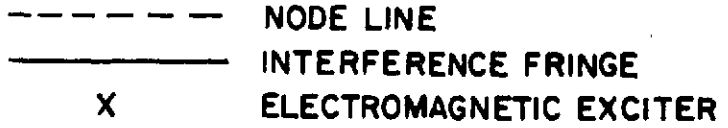
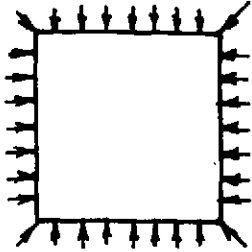


FIGURE II. PLATE MODES - 16 SUPPORT CONFIGURATIONS

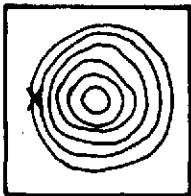
SUPPORT CONFIG.



Sketches of Real Time Observations

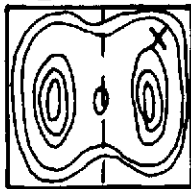
- NODE LINE
- INTERFERENCE FRINGE
- X ELECTROMAGNETIC EXCITER

#1

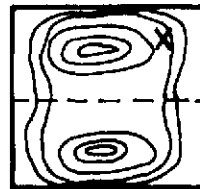


K=21.6
DOUBLY SYMMETRIC

#2

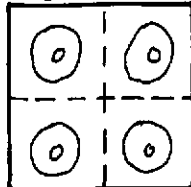


K=50.1
SYMMETRIC-ANTISYMMETRIC



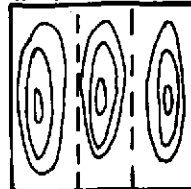
K=50.28

#3



K=75.4
DOUBLY ANTISYMMETRIC

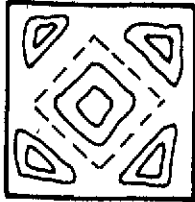
#4



K=88.1
SYMMETRIC-ANTISYMMETRIC

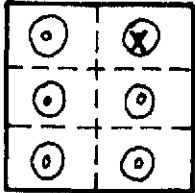
FIGURE 12. PLATE MODES-32 SUPPORT CONFIGURATION

#5

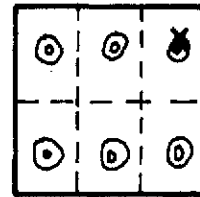


K=95.1
DOUBLY SYMMETRIC

#6

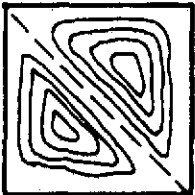


K=115.3
SYMMETRIC-ANTISYMMETRIC

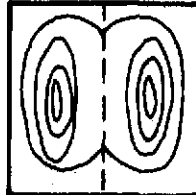


The following is a representation of the uncoupling of the first symmetric-antisymmetric mode.

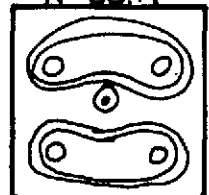
K=49.33



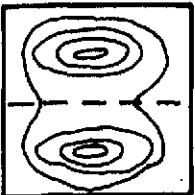
K=50.07



K=50.17



K=50.28



K=50.39

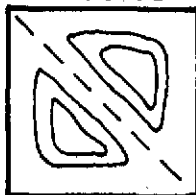
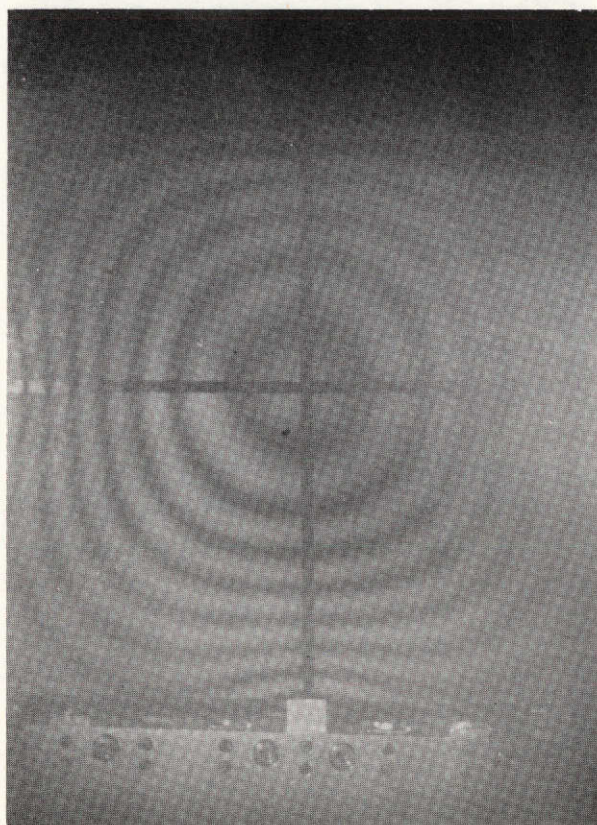


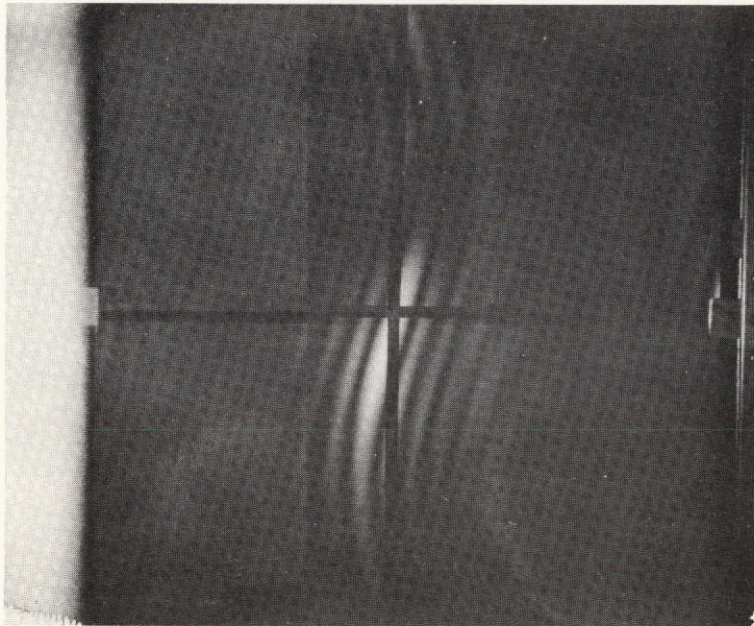
FIGURE 12. PLATE MODES—32 SUPPORT CONFIGURATION
(CONTINUED)

PHOTOGRAPHS OF TIME AVERAGE HOLOGRAMS



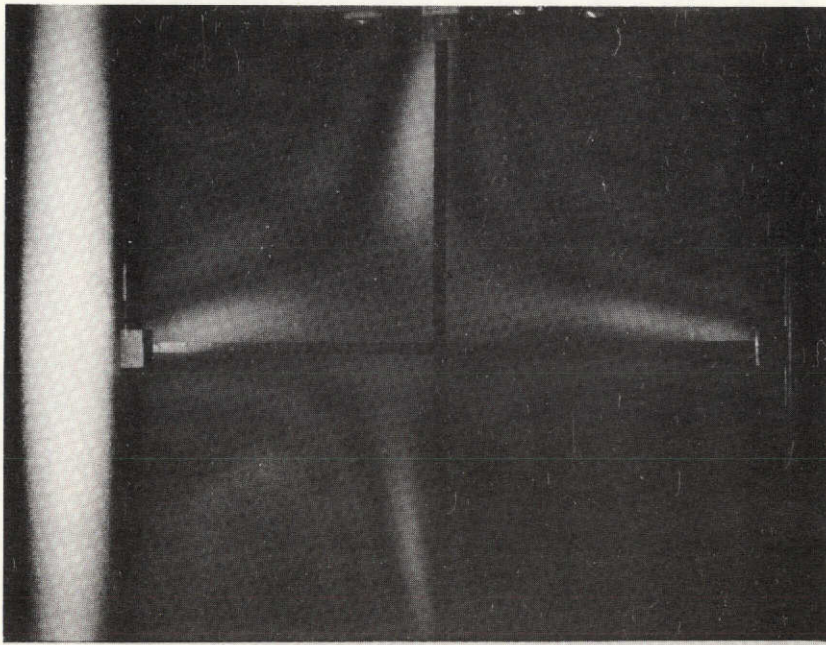
#1
K=19.6
DOUBLY SYMMETRIC

FIGURE 13d. PLATE MODES - 8 SUPPORT CONFIGURATION



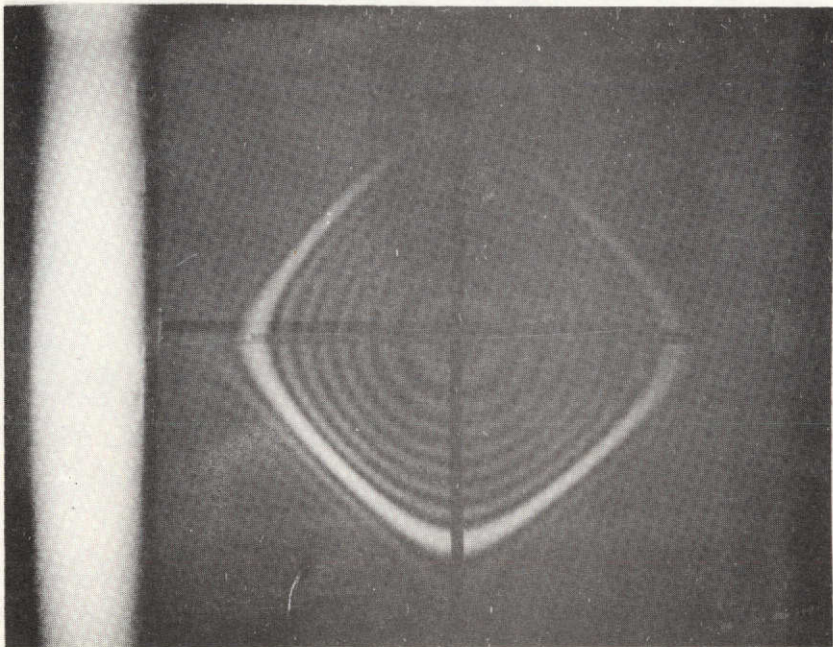
2
K=36.0
SYMMETRIC-ANTISYMMETRIC

FIGURE 13b. PLATE MODES — 8 SUPPORT CONFIGURATION



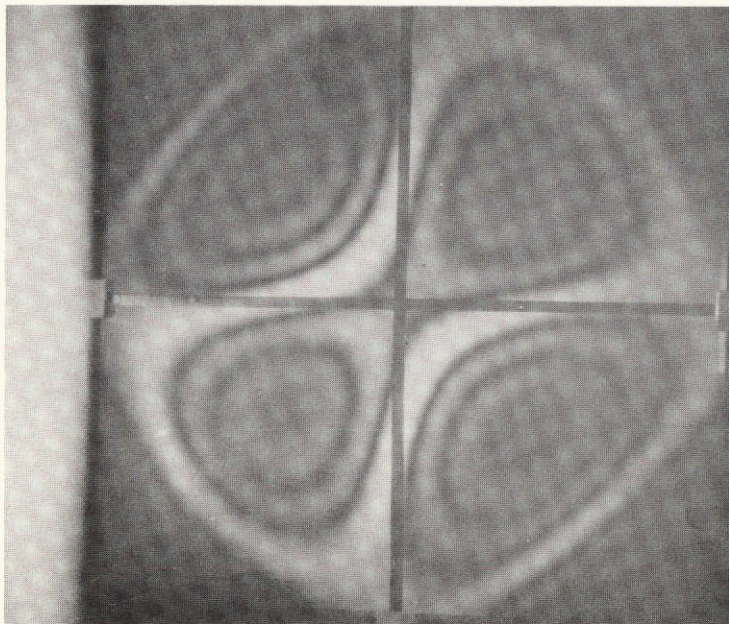
3
K = 39.9
DOUBLY ANTISYMMETRIC

FIGURE 13c. PLATE MODES— 8 SUPPORT CONFIGURATION



4
K=58.
DOUBLY SYMMETRIC

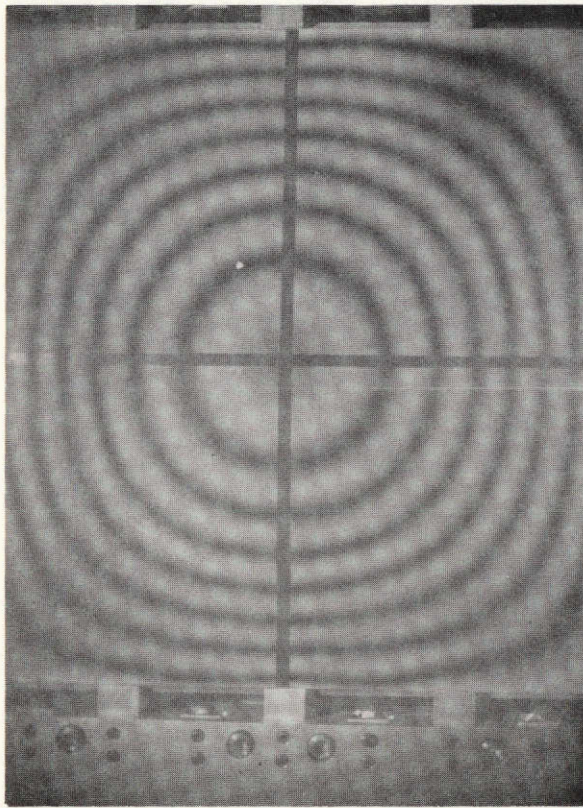
FIGURE 13d. PLATE MODES-8 SUPPORT CONFIGURATION



6
K=131.9
DOUBLY ANTISYMMETRIC

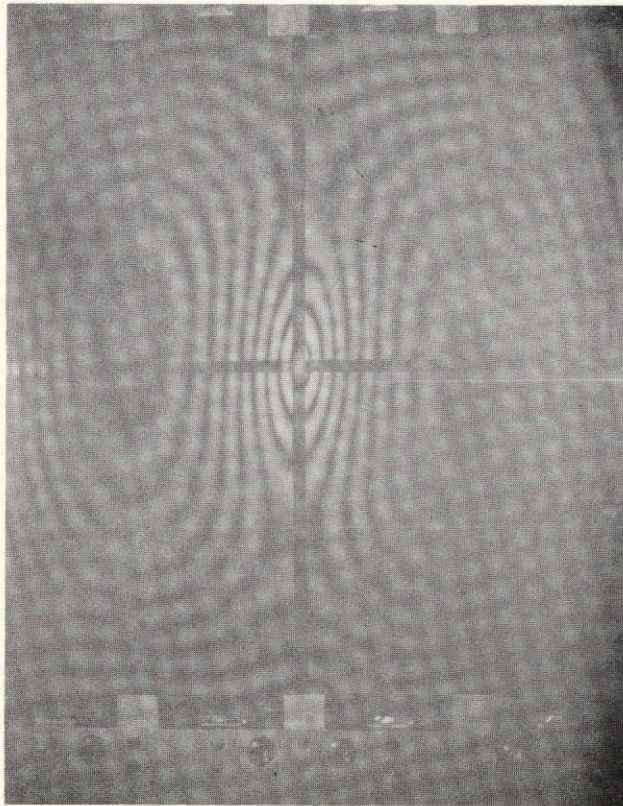
FIGURE 13e. PLATE MODES — 8 SUPPORT CONFIGURATION

PHOTOGRAPHS OF TIME AVERAGE HOLOGRAMS



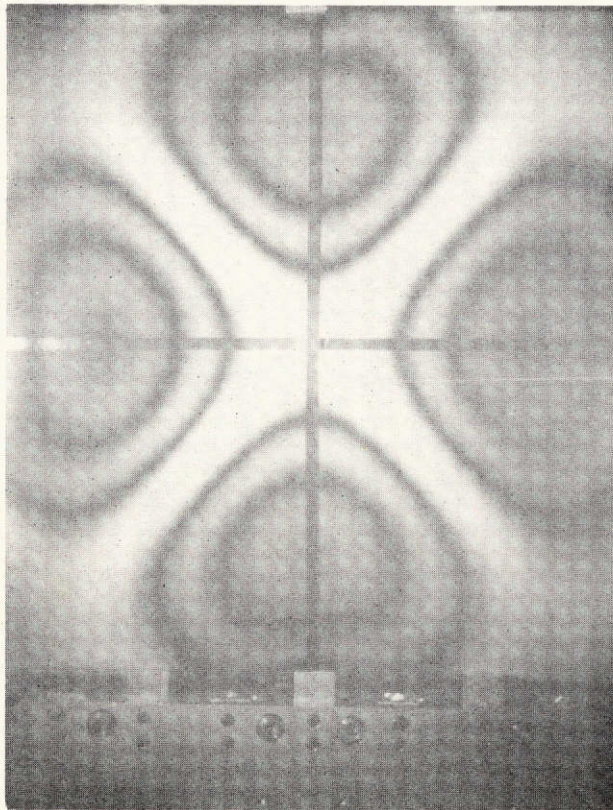
1
K=21.3
DOUBLY SYMMETRIC

FIGURE 14a. PLATE MODES - 16 SUPPORT CONFIGURATION



2
K = 49.
SYMMETRIC-ANTISYMMETRIC

FIGURE 14b. PLATE MODES - 16 SUPPORT CONFIGURATION

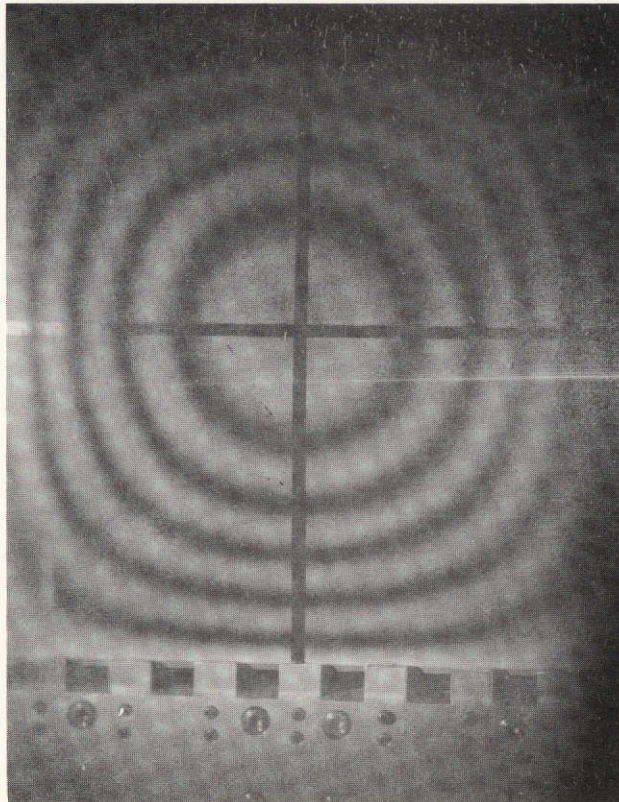


* $K=92.3$
DOUBLE SYMMETRIC

* THIS MODE WAS NOT SEEN DURING REAL TIME HOLOGRAPHY

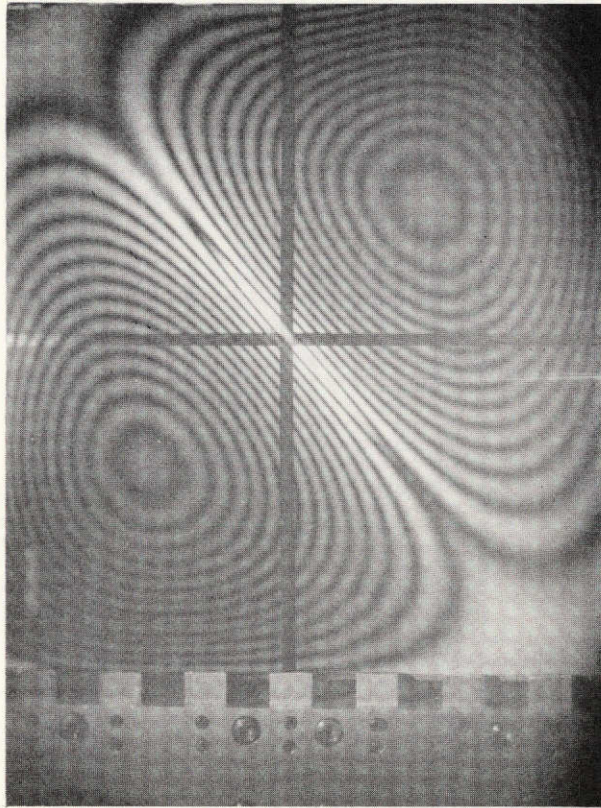
FIGURE 14c. PLATE MODES —16 SUPPORT CONFIGURATION

PHOTOGRAPHS OF TIME AVERAGE HOLOGRAMS



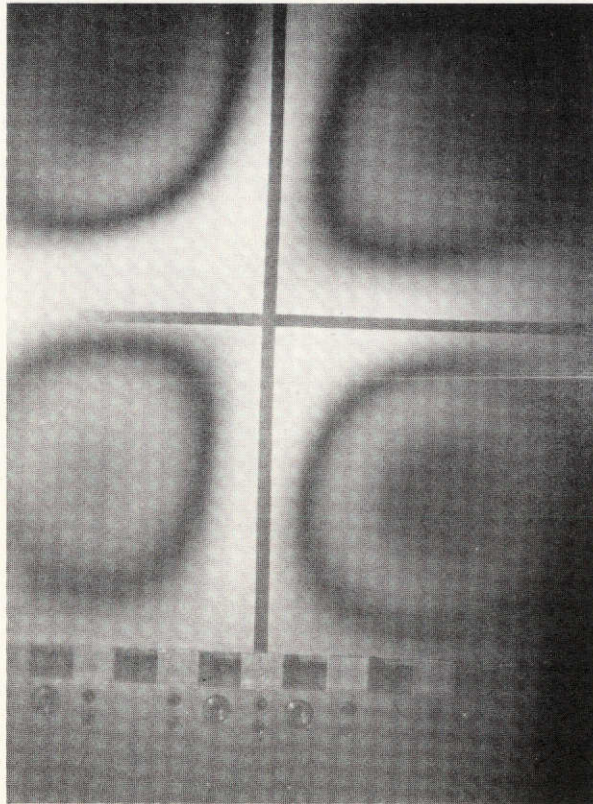
1
K = 21.1
DOUBLY SYMMETRIC

FIGURE 15a. PLATE MODES - 32 SUPPORT CONFIGURATION



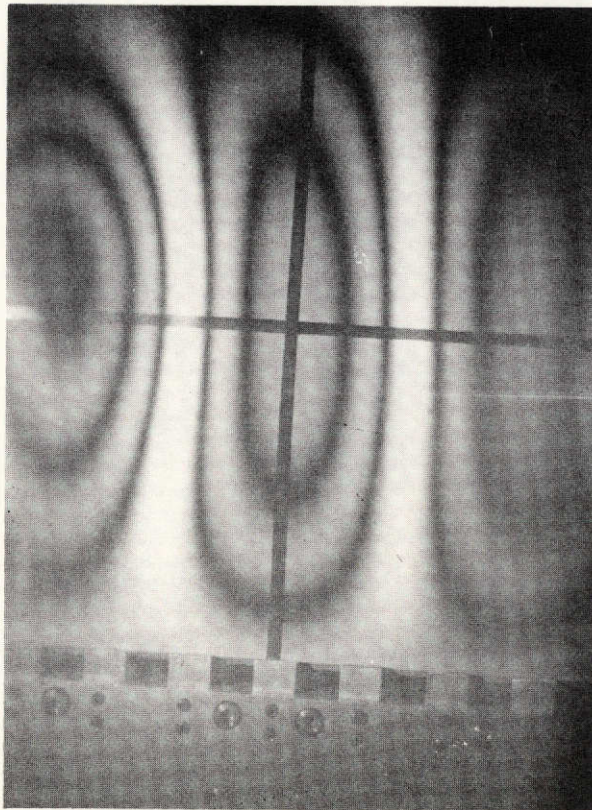
2
K=49.65 (COUPLED)
SYMMETRIC-ANTISYMMETRIC (UNCOUPLED)

FIGURE 15b. PLATE MODES—32 SUPPORT CONFIGURATION



3
K= 73.86
DOUBLY ANTISYMMETRIC

FIGURE 15c. PLATE MODES—32 SUPPORT CONFIGURATION



4
* K=94.96
SYMMETRIC-ANTISYMMETRIC

* NOTE FREQUENCY DIFFERENCE FROM REAL TIME OBSERVATION. MODE IS SOMEWHAT DISTORTED HOWEVER AND PERHAPS THIS IS THE CAUSE OF THE FREQUENCY DIFFERENCE.

FIGURE 15d. PLATE MODES-32 SUPPORT CONFIGURATION